Extending the Spin Excitation Lifetime of a Magnetic Molecule on a Proximitized Superconductor

Katerina Vaxevani, Jingcheng Li, Stefano Trivini, Jon Ortuzar, Danilo Longo, Dongfei Wang, and Jose Ignacio Pascual*

Cite This: https://doi.org/10.1021/acs.nanolett.2c00924

Read Online

ACCESS | Metrics & More | Article Recommendations | Supporting Information

ABSTRACT: Molecular spins on surfaces potentially used in quantum information processing and data storage require long spin excitation lifetimes. Normally, coupling of the molecular spin with the conduction electrons of metallic surfaces causes fast relaxation of spin excitations. However, the presence of superconducting **pairing** effects in the substrate can protect the excited spin from decaying. In this work, we show that a proximity-induced superconducting gold film can sustain spin excitations of a FeTPP-Cl molecule for more than 80 ns. This long value was determined by studying inelastic spin excitations of the S = 5/2 multiplet of FeTPP-Cl on Au films over V(100) using scanning tunneling spectroscopy. The spin lifetime decreases with increasing film thickness, along with the decrease of the effective superconducting gap. Our results elucidate the use of proximitized gold electrodes for addressing quantum spins on surfaces, envisioning new routes for tuning the value of their spin lifetime.

KEYWORDS: superconducting proximity effect, spin excitation lifetime, iron porphyrin, scanning tunneling microscopy
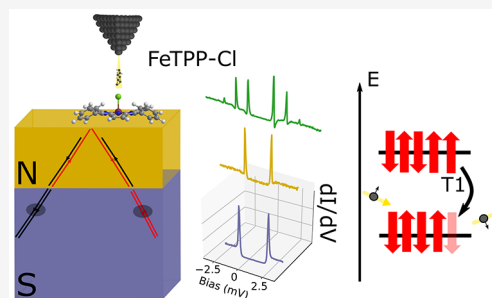
Magnetic molecules have been under the spotlight for new quantum applications, such as quantum information processing, sensing, and data storage.[1] Magnetic molecules can be tailored to behave as quantum bits (qubits), given that they exhibit long coherence (T_2) and spin-relaxation times (T_1).[2,3] The former is one major prerequisite for engineering efficient molecular qubits[4−6] as it describes the lifetime of their superposition state, while the latter gives the upper limit to T_2. Incorporating molecular spins on solid-state platforms is the next step toward creating electrically addressable quantum devices. However, the interaction with metallic electrodes opens fast decaying channels that dampen the spin dynamics. Thus, there is a need of finding metallic substrates for magnetic molecules that do not alter their spin dynamics while allowing electrical access.

Previous measurements on transition metal atoms on surfaces reported spin excitation lifetimes up to a few hundreds of picoseconds.[7−10] Inserting a Cu_2N decoupling layer over the metallic surface can enlarge the spin-relaxation lifetime to nanosecond time scales.[11] Another method to decouple spins from the electronic bath is to use a superconducting substrate. The energy gap around the Fermi level (E_F) can efficiently protect the spin excitations from decaying through generation of electron−hole pairs. For example, spin excitation lifetimes reaching ≈10 ns have been observed in a Fe-based porphyrin over a lead substrate.[12] Unfortunately, many elemental superconductors strongly hybridize with molecular species,

quenching their spin state, or simply are difficult to integrate into large scale devices.

Here, we took advantage of the proximity effect to induce a superconducting gap on a gold thin film[13−16] that extended the excitation lifetime of a tetraphenylporphyrin iron(III) chloride (FeTPP-Cl) for more than 80 ns. High quality gold films were epitaxially grown on top of the oxygen reconstructed 1×5-V(100) surface. We used a scanning tunneling microscope (STM) at 1.2 K to perform inelastic electron tunneling spectroscopy (IETS) on FeTPP-Cl molecules adsorbed on the Au/V(100) surface that revealed the existence of such very long spin excitation lifetimes. Moreover, we found that increasing the thickness of the gold layer resulted in a reduction of the excited-state lifetime, which coincided with the gradual shift down of the proximity-induced in-gap resonances. By approaching the STM tip to the molecules, we modified the magnetic coupling with the substrate to a stronger regime, where Yu−Shiba−Rusinov (YSR)[17−19] states appear inside the gap.[20]

Vanadium is a type-II superconductor with a critical temperature of T_c = 5.4 K. Vanadium single crystals contain impurities embedded in the bulk, namely, oxygen, carbon, and nitrogen.[21,22] In particular, the presence of oxygen creates a reconstructed V(100)-O(5×1) surface[23−26] persisting even
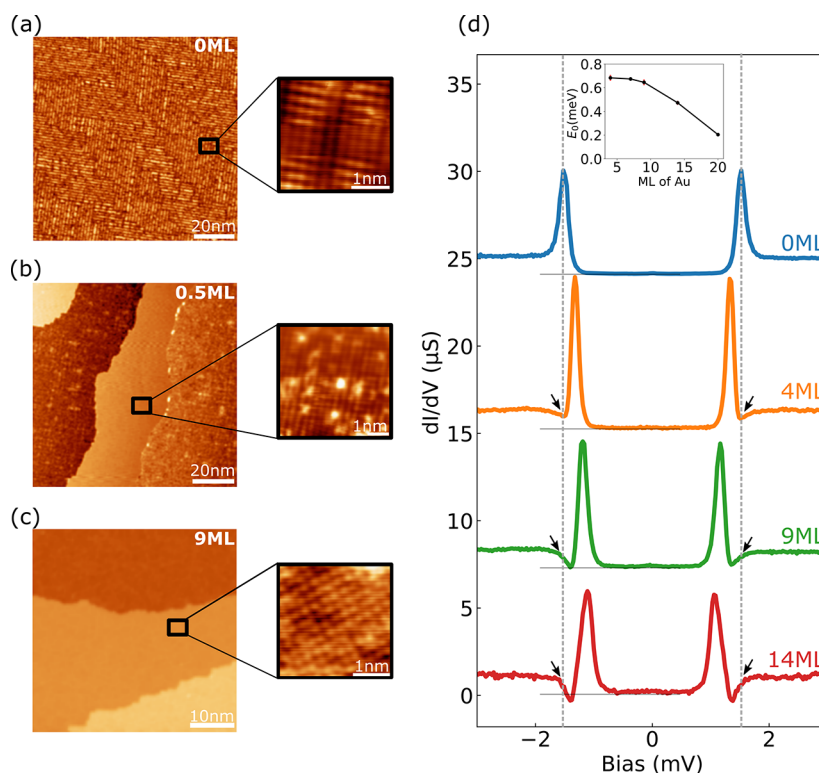
Figure 1. (a) STM image of the oxygen reconstructed 5×1-V(100) surface, where oxygen atoms occupy bridge positions along every fifth V atom row (as shown in inset): I = 1 nA; V = 700 mV (inset: I = 3 nA; V = 3 mV). (b) STM image after depositing 0.5 ML (I = 100 pA; V = −300 mV (inset: I = 100 pA; V = 5 mV)) and (c) 9 ML of Au on V(100)-O(5×1) (I = 100 pA; V = 1 V (inset: I = 400 pA; V = 50 mV)). (d) STS spectra (using a superconducting V-coated tip) on different numbers of Au layers on V(100)-O(5×1). Spectra have been shifted vertically for clarity. Horizontal line indicates zero conductance. Inset: evolution of the dGSJ intragap states compared to the amount of grown Au layers.

after very high temperature annealing (Figure 1a). Scanning tunneling spectroscopy (STS) measurements were performed to study the magnitude of the superconducting gap. To maximize the energy resolution, the tip was indented in the V sample to become superconducting.[27] Differential conductance (dI/dV) spectra on the V(100)-O(5×1) surface revealed two clear dI/dV peaks at V = ±1.5 mV (blue plot in Figure 1d), corresponding to tunneling between coherence peaks of tip and sample at V = ±(Δ_t + Δ_s), and in agreement with a gap value for bulk vanadium of $2\Delta_s \approx$ 1.5 meV.[28]

Molecular adsorption on bare V(100)[29] is challenging due to the high reactivity of the surface, which can distort molecular structure and its functionality. Therefore, we covered the vanadium surface with gold films, a metal typically employed for hosting molecular assemblies. We grew multiple gold layers on the V(100)-O(5×1) surface and studied the formation of superconducting pairing correlations through the proximity effect.[15,30] In Figure 1b,c, STM images show the epitaxial growth of gold on the V(100)-O(5×1) (herein referred to as V(100)) surface after annealing the substrate to 550 °C (see Methods). Atomic resolution images of the film lattice reveal a (100) surface orientation and lattice constant x = y ≈ 3 Å, compatible with that of the Au(100) surface, probably mixed with V atoms diffused through the film.[31]

STS measurements on the gold films showed that they maintain the superconducting character of the underlying V(100) crystal with a proximity-induced gap of width $2\Delta_s \approx$ 1.5 meV. For all film thicknesses explored in Figure 1d, spectra are characteristic of proximitized films thinner than the superconducting coherence length. They show shoulders

(black arrows in Figure 1d) close to ±(Δ_s + Δ_t), the convoluted gap of the vanadium bulk and tip, and a pair of sharp spectral resonances inside the proximity gap.[13,32] These resonances, first described by de Gennes and Saint-James,[33] are intragap quasiparticle excitation peaks resulting from Andreev reflections at the metal−superconductor interface.[32,34] The de Gennes−Saint-James resonances (dGSJ) shift down in energy with increasing film thickness, from 0.69 meV (4 monolayers (ML)) to 0.2 meV (20 ML) (see the Supporting Information[35]).

Next, we deposited FeTPP-Cl molecules on the Au/V(100) system. As previously reported,[36,37] deposition of FeTPP-Cl molecules on metallic substrates at room temperature usually results in coexistence of chlorinated and dechlorinated FeTPP species (Figure 2a). The chlorine atoms appear in STM topographic images as protrusions in the center of the molecules, whereas the dechlorinated FeTPP molecules show depressions at the center. Furthermore, as shown in Figure 2a, FeTPP-Cl appears with two distinctive adsorption geometries, referred to as 4-fold and 2-fold structures, due to the different apparent positions of the phenyl rings. The 4-fold species lie in a stronger interaction regime with the surface, which will be described elsewhere.[38] In contrast with previous results on Pb(111) and Au(111),[39−43] dechlorinated molecules on this substrate do not exhibit neither YSR in-gap states nor inelastic spin excitations outside the gap (Figure 2b), indicating that they may lie in a different coupling regime with the substrate.

In this letter, we focus on the 2-fold FeTPP-Cl molecules. Characteristic dI/dV curves recorded on the molecular center show excitation peaks outside the superconducting gap, at
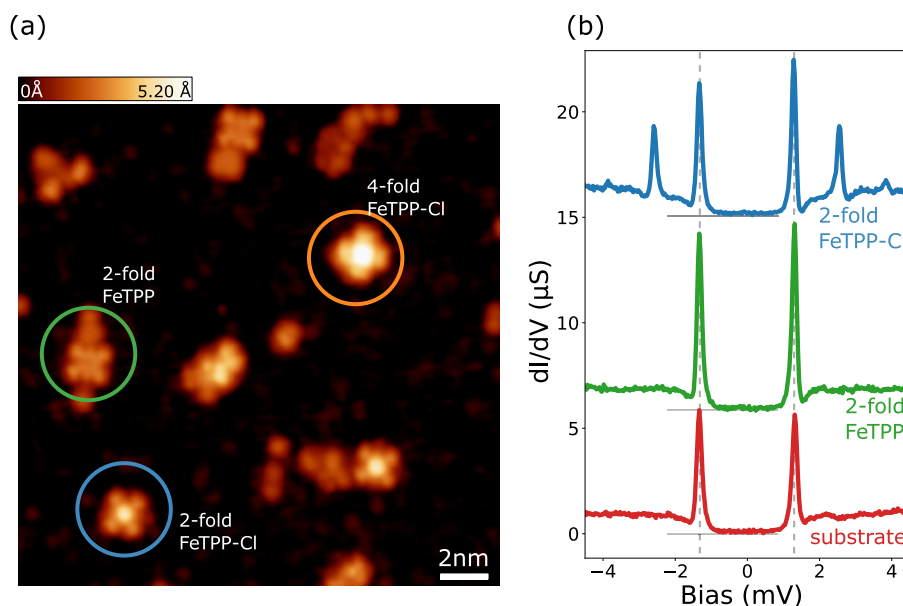
(a)

(b)

Figure 2. (a) STM image of 4-fold FeTPP-Cl (orange circle), 2-fold FeTPP-Cl (blue circle), and 2-fold FeTPP (green circle) on Au/V(100) (16 × 16 nm; I = 20 pA; V = 200 mV). (b) STS spectra of the different molecular species on Au/V(100) (I = 200 pA; V = 5 mV; spectra have been shifted for clarity; horizontal line indicates zero conductance).

≈±2.6 mV and ≈±3.8 mV (Figure 3a). These peaks have been previously attributed to inelastic excitations of the $S = 5/2$ molecular spin multiplet.[12,44] Using the phenomenological Hamiltonian $H = DS_z^2$ to describe the effect of a ligand field, a positive magnetic uniaxial anisotropy D found for these molecules splits the degenerate Fe multiplet into three spin states, $S_z = \pm|1/2\rangle$, $\pm|3/2\rangle$, and $\pm|5/2\rangle$.[4] The inelastic signal appears as a replica of the dGSJ peaks in the spectra, and the energy separation between them (red arrows in Figure 3a) corresponds to the excitation energies, that is, $2D$ from the ground state $S_z = \pm|1/2\rangle$ to the first excited state $S_z = \pm|3/2\rangle$ and $4D$ subsequently to the second excited state, $S_z = \pm|5/2\rangle$ (Figure 3c). Therefore, from these measurements we obtain that the axial magnetic anisotropy for FeTPP-Cl amounts to $D = 0.65$ meV. Due to the spin selection rule $\Delta S_z = \pm1$, the occupation of the second excited state can only be achieved from the first excited state.[9,12] The observation of a peak at $4D$ thus indicates that the first excited state reaches a finite population in a stationary state with the tunneling current.[12,44] Such stepwise excitation of higher lying spin states is referred to as spin-pumping.[9]

We studied the spin excitation dynamics of 2-fold molecules first on a 4 monolayer thick Au film on V(100), with characteristic spectra such as the one shown in Figure 3a. Interestingly, the excitation into the $S_z = \pm|5/2\rangle$ state is still observed for tunneling currents as small as 20 pA, suggesting a particularly long lifetime for the first excited state ($S_z = \pm|3/2\rangle$). The lifetime of the excited states, τ_i, can be extracted from the behavior of the IETS peaks with current, using a set of rate equations $\frac{dN_i}{dt} = \sum_j (R_{ji}N_j - R_{ij}N_i)$ connecting states N_i and N_j with excitation/de-excitation rates R_{ij} and R_{ji}.[12]

For the first excited state, the de-excitation rate R_{ji} includes a spontaneous decay constant, λ_1 and a current-induced de-excitation factor f (see the Supporting Information[35]). The former gives the lifetime of the first excited state ($\lambda_1 = 1/\tau_1$) and defines the threshold to a stationary non-equilibrium state.

In this regime, only the inelastic current drives transitions between the ground state and the first excited state, which dynamically acquires a finite population. This opens a new conduction channel for the second excited state.

To determine τ_1, we acquired multiple spectra similar to the one shown in Figure 3a with increasing set-point current. A stacked plot of distance-dependent dI/dV spectra is shown in Figure 3b, where we observe an increase in the intensity of the excitation peaks as the tip approaches the molecule. The ratio A_{r1} between the amplitude of the first excitation peak, A_1, and that of the coherence peaks, A_{BCS}, is plotted in Figure 3d (top panel) as a function of I_{BCS}, the current at the coherence peaks. The inelastic amplitude first increases with the tunneling rate and then stabilizes in a plateau characteristic of a stationary state. Fitting these data with rate equations from Heinrich et al.[12] yields a value of $\tau_1 \approx 80$ ns for FeTPP-Cl on 4 ML of Au on V(100) (see fitting procedures in the Supporting Information[35]). Such a large lifetime is attributed to the protection of the excited state by the superconducting gap, which forbids spin relaxation via creation of electron−hole excitations because $2D < 2\Delta_s$.

Interestingly, the value of τ_1 obtained for FeTPP-Cl on Au/V(100) is 8 times larger than the related molecule Fe-OEP-Cl on Pb(111),[12] where the de-excitation is protected by an even larger superconducting gap. As previously shown,[45,46] another possible decaying mechanism at sufficiently low temperatures is through the direct emission of resonant phonons, with energy $\omega\hbar \approx 2D$. The effectiveness of this relaxation mechanism depends strongly on the available phonon density at this energy and the intrinsic electron−phonon coupling of the material, as expressed in the Eliashberg coupling function.[47,48] Previous measurements of the phononic DOS and the calculated electron−phonon coupling of lead show a higher phonon density of states near the Fermi level compared with the one of vanadium or gold, and specifically around the related spin excitation energies.[49−51] Thus, since less available phonon states exist for the vanadium−gold system around the excitation energy, we speculate that this is a possible reason
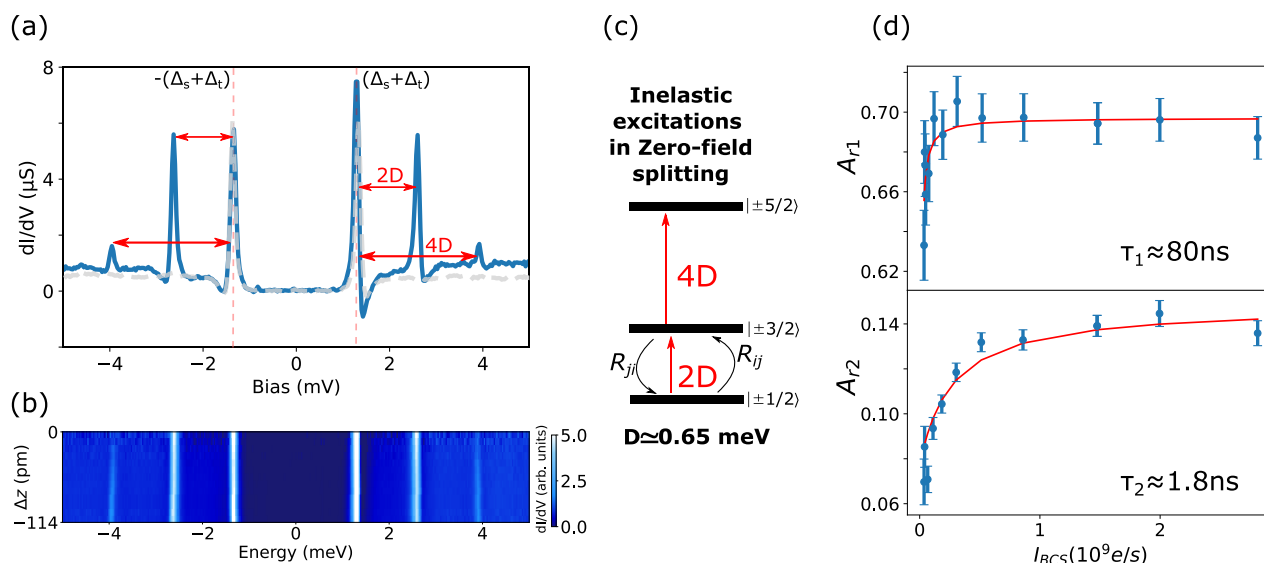
C

Figure 3. (a) Single STS spectra taken on a 2-fold FeTPP-Cl molecule (solid blue) and on the substrate (dashed gray) ($I = 150$ pA; $V = 6$ mV). (b) 2D intensity plot of a series of distance-dependent dI/dV spectra for 4 ML Au thickness. (c) Zero field splitting excitations for a total spin of $S_z = 5/2$. (d) Top (bottom) panel: Relative amplitude A_{r1} (A_{r2}) of the first (second) excitation resonance as a function of I_{BCS}, the current of the BCS peaks. Error bars indicate the error propagation of the relative amplitude averaged over positive and negative sides of the spectra. Top: Fit (red line) for determining the lifetime of the first excited state $\pm|3/2\rangle$ with thickness of 4 ML ($\tau_1 = 80 \pm 20$ ns), Bottom: Fit (red line) for determining the lifetime of the second excited state $\pm|5/2\rangle$ with thickness of 4 ML, with fixed τ_1 ($\tau_{2\rightarrow1} = 1.8 \pm 0.8$ ns).
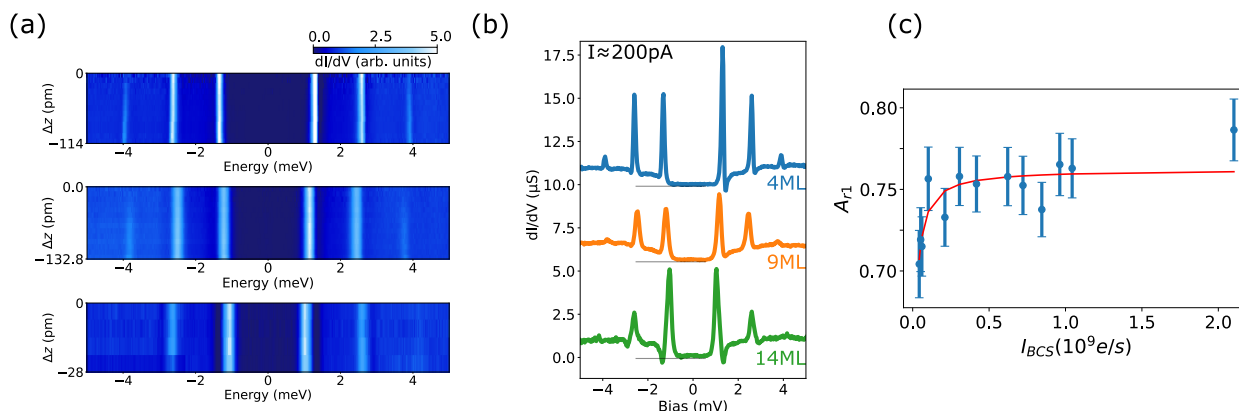

Figure 4. (a) 2D intensity plots of a series of distance-dependent dI/dV spectra for 4, 9, and 14 ML Au thicknesses on V(100). (b) Single STS spectra taken on a FeTPP-Cl molecule on 4 ML (blue), 9 ML (orange), and 14 ML (green) Au thicknesses on V(100) ($I = 200$ pA; $V = 6$ mV; spectra have been shifted vertically for clarity; horizontal line indicates zero conductance). (c) Fit for determining the lifetime of the first excited state $\pm|3/2\rangle$ with thickness of 9 ML ($\tau_1 = 39 \pm 10$ ns).

that explains the observed higher spin lifetimes in our experiments.

From the stacked spectra in Figure 3b, we can also obtain an estimation of the lifetime $\tau_{2\rightarrow1}$ of the second excited state $S_z = \pm|5/2\rangle$. In the bottom panel of Figure 3d, we plot the relative amplitude of the second excitation peak, A_{r2}, with respect to I_{BCS}. Fitting the data with a set of rate equations (red line) yields a value of $\tau_{2\rightarrow1} \lesssim 2$ ns (see the Supporting Information[35]). Electrons populating the second excited state have now sufficient energy ($4D > 2\Delta_s$) to directly decay into the substrate by electron−hole pair excitations, lowering the lifetime of the highest excited state. Nevertheless, this value is still relatively large and comparable to magnetic atoms on insulating films.[9]

To test the influence of the intragap bound states on the lifetimes of the excited states, we compared FeTPP-Cl spin excitation dynamics in samples with different Au thicknesses. In Figure 4a, two-dimensional intensity plots of a series of

distance-dependent dI/dV spectra for 4, 9, and 14 ML Au thicknesses are shown. The plots show the shift of the dGSJ resonances to lower energies as a function of the Au thickness, similar to Figure 1b.

We follow the same fitting procedure for determining the excited-state lifetime of FeTPP-Cl on every film thickness. For 9 ML, the fit yields a value of $\tau_1 = 39$ ns ±10 ns and $\tau_{2\rightarrow1} = 1.1$ ns ±2.2 ns for the lifetime of the first and second excited states, respectively (Figure 4c and Figure S2). On the 14 ML film, we could hardly observe faint second excitation peaks (Figure 4b) by approaching the tip to the closest possible position ($I = 200$ pA) before picking up the molecule. This determined an upper limit for the spin excitation of $\tau_1 < 1$ ns.

The reduction in excitation lifetime is in agreement with the gradual shift of the dGSJ resonances in the proximitized Au film. From Figure 1d, we obtain that the bound state values decrease from ∼0.69 meV (4 ML) to ∼0.65 meV (9 ML), and finally to ∼0.45 meV (14 ML). In contrast, the magnetic
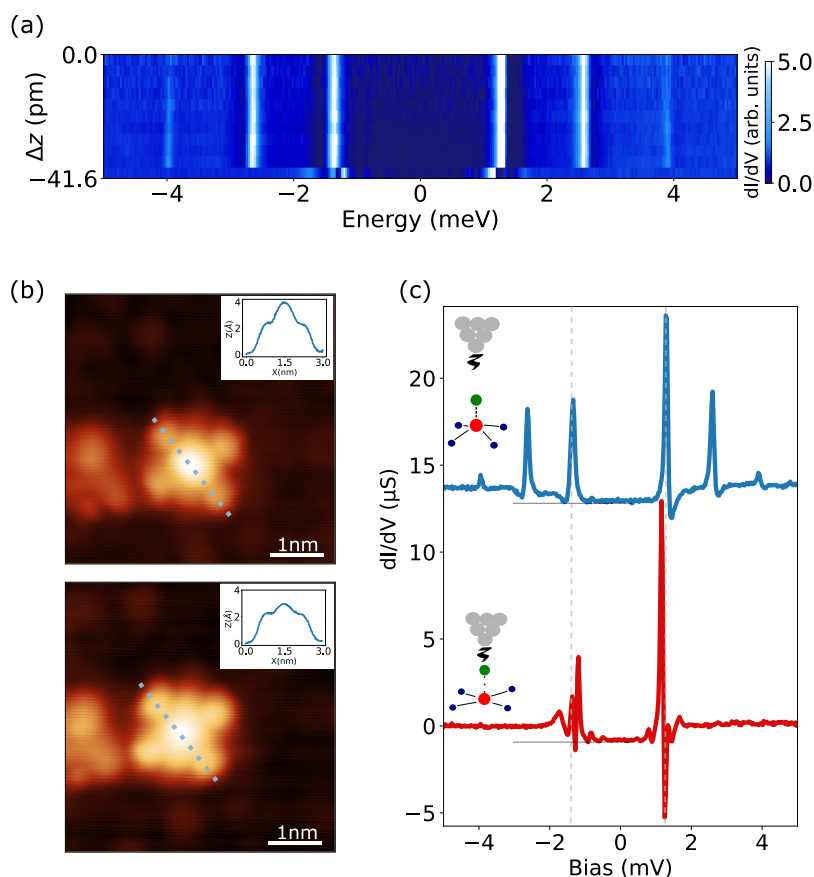
Figure 5. (a) 2D intensity plot of a series of distance-dependent dI/dV spectra for a switching FeTPP-Cl molecule. (b) STM images taken before (top) and after (bottom) the change of the interaction regime. Insets: line profiles taken across the molecule as indicated by the blue dotted line. (c) Single dI/dV spectra before (top, I = 400 pA; V = 6 mV;) and after (bottom, I = 450 pA; V = 6 mV;) the change of the interaction regime. Insets: Cartoon model representing the tip-induced effect far from (top) and close to (bottom) the molecule. Spectra have been shifted for clarity. Horizontal line indicates zero conductance.

anisotropy, as obtained from the position of the spectral peaks, V(100), while increasing to $D \approx 0.8$ meV for the 14 ML film. Variations in D have been previously observed in different magnetic systems on metallic substrates and attributed to either structural changes[12,52,53] or variations in the Kondo coupling with the substrate.[54] Comparing the spectra of FeTPP-Cl on the different gold thicknesses in Figure 4b, we note that the dGSJ peaks show a clear asymmetry for the 4 ML sample that decreases for 9 ML and vanishes for the 14 ML case. Such a spectral imbalance reflects a particle−hole asymmetry in the quasiparticle excitations of the super-conductor, probably due to the presence of a finite coupling with the molecule. The absence of peak asymmetry for the 14 ML reveals a significantly smaller Kondo coupling with the substrate, which can explain a renormalized magnetic anisotropy to a larger value.[55,56]

The weak adsorption regime of this molecular species could be irreversibly modified by approaching the tip beyond a specific distance. In this case, we observed an abrupt change in the dI/dV signal (Figure 5a). The two characteristic spin excitation peaks disappear, while two pairs of YSR states arise within the superconducting gap (Figure 5c, bottom spectra). The emergence of YSR states indicates the increase of the exchange coupling strength, J, of the molecular spin with the Cooper pairs of the superconducting condensate.[20] Such a change in the interaction regime, previously observed by Heinrich et al.,[57] is understood as a slight variation of the

molecular geometry induced by the tip in close proximity to the molecule. Attractive forces exerted to the Cl atom weaken the Cl−Fe bond and Fe is allowed to relax in the molecular plane, as shown in the cartoon of Figure 5c. In order to verify that this change of coupling regime is not due to the detachment of the Cl ligand, or any other irreversible molecular distortion, we compared STM images before and after the tip approach to find that the Cl atom remains intact (Figure 5b). Additionally, a broad peak emerges in the new regime outside the superconducting gap at $eV \approx 1.7$ mV. This new molecular configuration has been associated with a different oxidation state, with $S = 2$, stabilized by the hybridization of the Fe ion with the surface.[58]

In summary, in this work we have shown that proximity-induced superconducting gold thin films can enhance the spin excitation lifetime of magnetic molecules. We explored the spin excitation lifetimes of an $S = 5/2$ iron(III) porphyrin−chloride molecule on Au films grown on V(100) by implementing IETS with an STM. Our results found spin excitation lifetimes of ≈ 80 ns for the excitation of the $S_z = \pm 3/2$ multiplet, which is protected from decaying to an electron−hole pair excitation by the absolute proximity-induced gap of the substrate. The excitation lifetime in this surface platform is even larger than the one found for related species on Pb(111).[12] This is attributed to the lower density of phononic states in the substrate, suggesting that direct phonon emission is a lifetime limiting process. However, we also determined that the lifetime

is affected by a pair of in-gap de Gennes—Saint-James resonances in the film, which separate from the gap edge and shift inward toward zero energy, thus opening alternative (coherent) channels for decaying. Overall, the Au/V(100) platform offers the advantage of employing a noble metal, mild in molecular adsorption and reactions, for studies of long spin dynamics. Additionally, the presence of coherent subgap states in the proximitized metal film suggests new potential methods for addressing spin states and excitations of magnetic molecules.

METHODS

All experiments were carried out in a commercial ultrahigh vacuum (UHV) scanning tunneling microscope of SPECS with a Joule-Thomson cooling stage reaching a base temperature of 1.2 K. For the acquired STS spectra, an external lock-in was used with a modulation frequency of 938 Hz and an amplitude of $V_{rms} = 20-50$ μV.

The vanadium (100) crystal used in this project was repeatedly sputtered with Ar^+ at 1.5 kV in UHV conditions ($P = 5 \times 10^{-9}$ mbar) and annealed at high temperatures (~1000 °C) in an attempt to remove the residual impurities as suggested by Kralj et al.[24] Gold thin films were deposited on V(100) with an e-beam evaporator. Afterward, the samples were postannealed for 10 min at 550 °C. The calibration of the deposition rate was made by evaporating 0.5 monolayer and subsequently checking the Au coverage by STM.

The tip was prepared by indenting up to 20 nm into the substrate. A superconducting tip results in a substantial increase of the energy resolution, since tunneling of electrons takes place between the two sharp DOS of tip and sample.[27] Sublimation of FeTPP-Cl molecules from a Knudsen cell at 297 °C resulted in a mixture of FeTPP-Cl and FeTPP species on the surface, shown in Figure 2.

ASSOCIATED CONTENT

Ⓢ Supporting Information

The Supporting Information is available free of charge at https://pubs.acs.org/doi/10.1021/acs.nanolett.2c00924.

Deconvolution of acquired dI/dV spectra for different Au thicknesses on V(100), as well as fit for energies of intragap states based on the de Gennes and Saint-James[33] model; rate equations leading to the fitting function for A_{r1} and A_{r2} and the fit for extracting the lifetime of the second excited state of the sample with 9 ML of Au; magnetic field dependent measurement (PDF)

AUTHOR INFORMATION

Corresponding Author

Jose Ignacio Pascual — *CIC nanoGUNE-BRTA, 20018 Donostia-San Sebastián, Spain; Ikerbasque, Basque Foundation for Science, 48013 Bilbao, Spain;* ⓞ orcid.org/0000-0002-7152-4747; Email: ji.pascual@nanogune.eu

Authors

Katerina Vaxevani — *CIC nanoGUNE-BRTA, 20018 Donostia-San Sebastián, Spain;* ⓞ orcid.org/0000-0003-1481-4446

Jingcheng Li — *CIC nanoGUNE-BRTA, 20018 Donostia-San Sebastián, Spain; School of Physics, Sun Yat-sen University, Guangzhou 510275, China*

Stefano Trivini — *CIC nanoGUNE-BRTA, 20018 Donostia-San Sebastián, Spain*

Jon Ortuzar — *CIC nanoGUNE-BRTA, 20018 Donostia-San Sebastián, Spain*

Danilo Longo — *CIC nanoGUNE-BRTA, 20018 Donostia-San Sebastián, Spain*

Dongfei Wang — *CIC nanoGUNE-BRTA, 20018 Donostia-San Sebastián, Spain;* ⓞ orcid.org/0000-0003-4645-2881

Complete contact information is available at:
https://pubs.acs.org/10.1021/acs.nanolett.2c00924

Notes

The authors declare no competing financial interest.

REFERENCES

(1) Gaita-Arino, A.; Luis, F.; Hill, S.; Coronado, E. Molecular spins for quantum computation. *Nat. Chem.* **2019**, *11*, 301−309.

(2) Ardavan, A.; Rival, O.; Morton, J. J. L.; Blundell, S. J.; Tyryshkin, A. M.; Timco, G. A.; Winpenny, R. E. P. Will Spin-Relaxation Times in Molecular Magnets Permit Quantum Information Processing? *Phys. Rev. Lett.* **2007**, *98*, 057201.

(3) Moreno-Pineda, E.; Godfrin, C.; Balestro, F.; Wernsdorfer, W.; Ruben, M. Molecular spin qudits for quantum algorithms. *Chem. Soc. Rev.* **2018**, *47*, 501−513.

(4) Gatteschi, D.; Sessoli, R.; Villain, J. *Molecular Nanomagnets*; Oxford University Press, 2006.

(5) Affronte, M. Molecular nanomagnets for information technologies. *J. Mater. Chem.* **2009**, *19*, 1731−1737.

(6) Sieklucka, B.; Pinkowicz, D. *Molecular Magnetic Materials: Concepts and Applications*; Wiley-VCH, 2016.

(7) Khajetoorians, A. A.; Lounis, S.; Chilian, B.; Costa, A. T.; Zhou, L.; Mills, D. L.; Wiebe, J.; Wiesendanger, R. Itinerant Nature of Atom-Magnetization Excitation by Tunneling Electrons. *Phys. Rev. Lett.* **2011**, *106*, 037205.

(8) Khajetoorians, A. A.; Schlenk, T.; Schweflinghaus, B.; dos Santos Dias, M.; Steinbrecher, M.; Bouhassoune, M.; Lounis, S.; Wiebe, J.; Wiesendanger, R. Spin Excitations of Individual Fe Atoms on Pt(111): Impact of the Site-Dependent Giant Substrate Polarization. *Phys. Rev. Lett.* **2013**, *111*, 157204.

(9) Loth, S.; von Bergmann, K.; Ternes, M.; Otte, A. F.; Lutz, C. P.; Heinrich, A. J. Controlling the state of quantum spins with electric currents. *Nat. Phys.* **2010**, *6*, 340−344.

(10) Hermenau, J.; Ternes, M.; Steinbrecher, M.; Wiesendanger, R.; Wiebe, J. Long Spin-Relaxation Times in a Transition-Metal Atom in Direct Contact to a Metal Substrate. *Nano Lett.* **2018**, *18*, 1978−1983.

(11) Loth, S.; Etzkorn, M.; Lutz, C. P.; Eigler, D. M.; Heinrich, A. J. Measurement of Fast Electron Spin Relaxation Times with Atomic Resolution. *Science* **2010**, *329*, 1628−1630.

(12) Heinrich, B. W.; Braun, L.; Pascual, J. I.; Franke, K. J. Protection of excited spin states by a superconducting energy gap. *Nat. Phys.* **2013**, *9*, 765−768.

(13) Truscott, A. D.; Dynes, R. C.; Schneemeyer, L. F. Scanning Tunneling Spectroscopy of NbSe$_2$-Au Proximity Junctions. *Phys. Rev. Lett.* **1999**, *83*, 1014−1017.

(14) Gupta, A. K.; Crétinon, L.; Moussy, N.; Pannetier, B.; Courtois, H. Anomalous density of states in a metallic film in proximity with a superconductor. *Phys. Rev. B* **2004**, *69*, 104514.

(15) Island, J. O.; Gaudenzi, R.; De Bruijckere, J.; Burzurí, E.; Franco, C.; Mas-Torrent, M.; Rovira, C.; Veciana, J.; Klapwijk, T. M.; Aguado, R.; Van Der Zant, H. S. Proximity-Induced Shiba States in a Molecular Junction. *Phys. Rev. Lett.* **2017**, *118*, 117001.

(16) Wei, P.; Manna, S.; Eich, M.; Lee, P.; Moodera, J. Superconductivity in the Surface State of Noble Metal Gold and its Fermi Level Tuning by EuS Dielectric. *Phys. Rev. Lett.* **2019**, *122*, 247002.

(17) Yu, L. Bound state in superconductors with paramagnetic impurities. *Acta. Phys. Sin.* **1965**, *21*, 75−91.

(18) Shiba, H. Classical Spins in Superconductors. *Prog. Theor. Phys.* **1968**, *40*, 435−451.

(19) Rusinov, A. I. On the Theory of Gapless Superconductivity in Alloys Containing Paramagnetic Impurities. *Sov. J. Exp. Theor. Phys.* **1969**, *29*, 1101.

(20) Heinrich, B. W.; Pascual, J. I.; Franke, K. J. Single magnetic adsorbates on s -wave superconductors. *Prog. Surf. Sci.* **2018**, *93*, 1−19.

(21) Wexler, A.; Corak, W. S. Superconductivity of Vanadium. *Phys. Rev.* **1952**, *85*, 85−90.

(22) Valla, T.; Pervan, P.; Milun, M. Photoelectron spectroscopy characterization of the V(100) surface. *Surf. Sci.* **1994**, *307−309*, 843−847.

(23) Koller, R.; Bergermayer, W.; Kresse, G.; Hebenstreit, E.; Konvicka, C.; Schmid, M.; Podloucky, R.; Varga, P. The structure of the oxygen induced (1×5) reconstruction of V(100). *Surf. Sci.* **2001**, *480*, 11−24.

(24) Kralj, M.; Pervan, P.; Milun, M.; Wandelt, K.; Mandrino, D.; Jenko, M. HRAES, STM and ARUPS study of (5×1) reconstructed V(100). *Surf. Sci.* **2003**, *526*, 166−176.

(25) Konvicka, C.; Hammerschmid, A.; Schmid, M.; Varga, P. Stabilizing single metal adatoms at room temperature: Pd on C- and O-covered V(100). *Surf. Sci.* **2002**, *496*, 209−220.

(26) Bischoff, M. M. J.; Konvicka, C.; Quinn, A. J.; Schmid, M.; Redinger, J.; Podloucky, R.; Varga, P.; van Kempen, H. Scanning tunneling spectroscopy on clean and contaminated V(001). *Surf. Sci.* **2002**, *513*, 9−25.

(27) Pan, S. H.; Hudson, E. W.; Davis, J. C. Vacuum tunneling of superconducting quasiparticles from atomically sharp scanning tunneling microscope tips. *Appl. Phys. Lett.* **1998**, *73*, 2992−2994.

(28) Huang, H.; Drost, R.; Senkpiel, J.; Padurariu, C.; Kubala, B.; Yeyati, A. L.; Cuevas, J. C.; Ankerhold, J.; Kern, K.; Ast, C. R. Quantum phase transitions and the role of impurity-substrate hybridization in Yu-Shiba-Rusinov states. *Commun. Phys.* **2020**, *3*, 199.

(29) Etzkorn, M.; Eltschka, M.; Jack, B.; Ast, C. R.; Kern, K. Mapping of Yu-Shiba-Rusinov states from an extended scatterer. *arXiv Preprint (Superconductivity)*, 2018. arXiv.1807.00646. https://arxiv.org/abs/1807.00646 (accessed 2022-02-21).

(30) Beck, P.; Schneider, L.; Bachmann, L.; Wiebe, J.; Wiesendanger, R. Structural and superconducting properties of ultrathin Ir films on Nb(110). *Phys. Rev. Mater.* **2022**, *6*, 024801.

(31) Naftel, S.; Bzowski, A.; Sham, T. Study of the electronic structure of A-V bimetallics using X-ray photoelectron spectroscopy (XPS) and X-ray absorption near-edge structure (XANES). *J. Alloys Compd.* **1999**, *283*, 5−11.

(32) Arnold, G. B. Theory of thin proximity-effect sandwiches. *Phys. Rev. B* **1978**, *18*, 1076−1100.

(33) de Gennes, P.; Saint-James, D. Elementary excitations in the vicinity of a normal metal-superconducting metal contact. *Phys. Lett.* **1963**, *4*, 151−152.

(34) Wolf, E. L.; Arnold, G. B. Proximity electron tunneling spectroscopy. *Phys. Rep.* **1982**, *91*, 31−102.

(35) See the Supporting Information.

(36) Gopakumar, T. G.; Tang, H.; Morillo, J.; Berndt, R. Transfer of Cl Ligands between Adsorbed Iron Tetraphenylporphyrin Molecules. *J. Am. Chem. Soc.* **2012**, *134*, 11844−11847.

(37) Heinrich, B. W.; Ahmadi, G.; Muller, V. L.; Braun, L.; Pascual, J.; Franke, K. J. Change of the magnetic coupling of a metal-organic complex with the substrate by a stepwise ligand reaction. *Nano Lett.* **2013**, *13*, 4840−4843.

(38) Trivini, S.; Ortuzar, J.; Vaxevani, K.; Li, J.; Bergeret, F. S.; Cazalilla, A. M.; Pascual, J. I. Pair excitations of a quantum spin on a proximitized superconductor. *arXiv Preprint (Superconductivity)*, 2022,. arXiv.2207.00617.

(39) Farinacci, L.; Ahmadi, G.; Reecht, G.; Ruby, M.; Bogdanoff, N.; Peters, O.; Heinrich, B. W.; Von Oppen, F.; Franke, K. J. Tuning the Coupling of an Individual Magnetic Impurity to a Superconductor: Quantum Phase Transition and Transport. *Phys. Rev. Lett.* **2018**, *121*, 196803.

(40) Farinacci, L.; Ahmadi, G.; Ruby, M.; Reecht, G.; Heinrich, B. W.; Czekelius, C.; Von Oppen, F.; Franke, K. J. Interfering Tunneling Paths through Magnetic Molecules on Superconductors: Asymmetries of Kondo and Yu-Shiba-Rusinov Resonances. *Phys. Rev. Lett.* **2020**, *125*, 256805.

(41) Rubio-Verdú, C.; Zaldivar, J.; Zitko, R.; Pascual, J. I. Coupled Yu-Shiba-Rusinov States Induced by a Many-Body Molecular Spin on a Superconductor. *Phys. Rev. Lett.* **2021**, *126*, 017001.

(42) Rubio-Verdú, C.; Sarasola, A.; Choi, D.-J.; Majzik, Z.; Ebeling, R.; Calvo, M. R.; Ugeda, M. M.; Garcia-Lekue, A.; Sanchez-Portal, D.; Pascual, J. I. Orbital-selective spin excitation of a magnetic porphyrin. *Commun. Phys.* **2018**, *1*, 15.

(43) Rubio Verdú, C. *Atomic-scale limits of magnetism and superconductivity explored by electron excitations in tunneling spectroscopy*. Ph.D. thesis, Universidad del Pais Vasco/Euskal Herriko Unibertsitatea (UPV/EHU), Leioa, Spain, 2019.

(44) Berggren, P.; Fransson, J. Theory of spin inelastic tunneling spectroscopy for superconductor-superconductor and superconductor-metal junctions. *Phys. Rev. B* **2015**, *91*, 205438.

(45) Astner, T.; Gugler, J.; Angerer, A.; Wald, S.; Putz, S.; Mauser, N. J.; Trupke, M.; Sumiya, H.; Onoda, S.; Isoya, J.; Schmiedmayer, J.; Mohn, P.; Majer, J. Solid-state electron spin lifetime limited by phononic vacuum modes. *Nat. Mater.* **2018**, *17*, 313−317.

(46) Liddle, S.; van Slageren, J. Improving f-element single molecule magnets. *Chem. Soc. Rev.* **2015**, *44*, 6655−6669.

(47) Eliashberg, G. M. Interactions between electrons and lattice vibrations in a superconductor. *Sov. Phys. - JETP (Engl. Transl.)* **1960**, *11*, 3.

(48) Hofmann, P.; Sklyadneva, I. Y.; Rienks, E. D. L.; Chulkov, E. V. Electron−phonon coupling at surfaces and interfaces. *New J. Phys.* **2009**, *11*, 125005.

(49) Delaire, O.; Kresch, M.; Muñoz, J. A.; Lucas, M. S.; Lin, J. Y. Y.; Fultz, B. Electron-phonon interactions and high-temperature thermodynamics of vanadium and its alloys. *Phys. Rev. B* **2008**, *77*, 214112.

(50) Lee, W.-J.; Ju, S.-P.; Sun, S.-J.; Weng, M.-H. Dynamical behaviour of 7−1 gold nanowire under different axial tensile strains. *Nanotechnology* **2006**, *17*, 3253−3258.

(51) Rowell, J. M.; McMillan, W. L.; Feldmann, W. L. Phonon Spectra in Pb and Pb$_{40}$Tl$_{60}$ Determined by Tunneling and Neutron Scattering. *Phys. Rev.* **1969**, *178*, 897−899.

(52) Heinrich, B. W.; Braun, L.; Pascual, J. I.; Franke, K. J. Tuning the Magnetic Anisotropy of Single Molecules. *Nano Lett.* **2015**, *15*, 4024−4028.

(53) Kezilebieke, S.; Zitko, R.; Dvorak, M.; Ojanen, T.; Liljeroth, P. Observation of Coexistence of Yu-Shiba-Rusinov States and Spin-Flip Excitations. *Nano Lett.* **2019**, *19*, 4614−4619.

(54) Oberg, J. C.; Calvo, M. R.; Delgado, F.; Moro-Lagares, M.; Serrate, D.; Jacob, D.; Fernandez-Rossier, J.; Hirjibehedin, C. F. Control of single-spin magnetic anisotropy by exchange coupling. *Nat. Nanotechnol.* **2014**, *9*, 64−68.

(55) Delgado, F.; Hirjibehedin, C.; Fernandez-Rossier, J. Consequences of Kondo exchange on quantum spins. *Surf. Sci.* **2014**, *630*, 337−342.

(56) Jacob, D. Renormalization of single-ion magnetic anisotropy in the absence of Kondo effect. *Phys. Rev. B* **2018**, *97*, 075428.

(57) Heinrich, B. W.; Ehlert, C.; Hatter, N.; Braun, L.; Lotze, C.; Saalfrank, P.; Franke, K. J. Control of Oxidation and Spin State in a Single-Molecule Junction. *ACS Nano* **2018**, *12*, 3172−3177.

(58) Uzma, F.; Yang, L.; He, D.; Wang, X.; Hu, S.; Ye, L.; Zheng, X.; Yan, Y. Understanding the Sub-meV Precision-Tuning of Magnetic Anisotropy of Single-Molecule Junction. *J. Phys. Chem. C* **2021**, *125*, 6990−6997.